Exchange Currents in Photoproduction of Baryon Resonances

U. Meyer¹, A.J. Buchmann, and Amand Faessler

Institute for Theoretical Physics, University of Tübingen Auf der Morgenstelle 14, D-72076 Tübingen, Germany

Abstract

We calculate photoexcitation amplitudes for all nucleon and Δ resonances up to \sqrt{s} =1.6 GeV. We use a chiral quark model including two-body exchange currents. The two-body currents give important contributions. For the $\Delta(1232)$ and the D₁₃(1520) we observe that the individual exchange current contributions considerably cancel each other while for the P₁₁(1440), the P₃₃(1600), and the S₁₁(1535) we get a reinforcement of the two-body amplitudes. In comparison with present experimental data, we obtain both for the S₁₁(1535) and for the P₁₁(1440) amplitudes an improvement with respect to the impulse approximation.

PACS numbers: 13.60.Rj, 13.40.Gp, 12.39.Pn, 14.20.Gk

Keywords: Photoexcitation amplitudes, chiral quark model, current conservation, two-body exchange currents, baryon resonances.

¹Supported by the DFG Graduiertenkolleg MU 705/3

The study of electro-and photocouplings of nucleon resonances gives insight into the internal structure of these resonances and is therefore important for our understanding of low-energy quark dynamics. The simultaneous description of the baryon mass spectrum and of electromagnetic (e.m.) transition amplitudes is certainly a more severe test for the quark-quark interaction than a description of the mass spectrum alone.

From the experimental side, with the construction of continuous wave electron accelerators, new and more exact data for nucleon resonance masses, widths, and photocouplings are expected to be obtained in the next years. The accuracy and statistics of these data will be comparable to those of hadronic processes [1].

From the theoretical side, the e.m. excitation of the nucleon has mostly been studied in the quark model [2-9]. We also use in the present calculations a Chiral Quark Potential Model (χ QPM). In the simple nonrelativistic quark model [3,5] the description of photoexcitation amplitudes has only partly been satisfactory. One reason might be the neglect of relativistic corrections in the single-quark current operator. These have been investigated e.g. in Refs.[4,7,8] and have in some cases led to a better agreement with the data. Another reason might be that most calculations have been done in the so-called impulse approximation where the whole photon four-momentum is transferred to one single constituent of the baryon, the other two quarks being spectators in the photon absorption process. However, in order to formulate a gauge invariant model, it has been known for a long time that it is necessary to take into account two-body exchange currents [10].

Two-body exchange currents have been shown to be important for quantities such as the neutron charge radius [11] or the magnetic moments of the nucleon [12] and the entire baryon octet [13]. In addition, they play an important role for the photoexcitation of the two lightest resonances, namely the Δ -isobar $(P_{33}(1232))$ [14] and the Roper resonance $(P_{11}(1440))$ [15]. We found that for the Roper resonance the inclusion of two-body currents slightly improves the agreement with experimental data. A similar improvement does not occur for the M1 transition amplitude of the Δ -isobar where the various exchange current contributions nearly completely cancel each other [14,15]. In this work we extend our study of the effect of two-body currents on photoproduction amplitudes of nucleon resonances by considering all excitations up to \sqrt{s} =1.6 GeV in order to investigate further whether the differences between quark model calculations and experimental values arise from the non-completeness of the e.m. current, i.e. from the neglect of two-body contributions.

The Hamiltonian of the χQPM is in the case of equal constituent quark masses m_q given by [13]

$$H = \sum_{i=1}^{3} \left(m_q + \frac{\mathbf{p}_i^2}{2m_q}\right) - \frac{\mathbf{P}^2}{6m_q} + \sum_{i < j}^{3} \left(V^{conf}(\mathbf{r}_i, \mathbf{r}_j) + V^{OPEP}(\mathbf{r}_i, \mathbf{r}_j) + V^{OSEP}(\mathbf{r}_i, \mathbf{r}_j) + V^{OGEP}(\mathbf{r}_i, \mathbf{r}_j)\right) . \tag{1}$$

Here, $\mathbf{p}_i(\mathbf{r}_i)$ describes the momentum (position) of the *i*-th constituent and \mathbf{P} the center of mass momentum, respectively. The interaction between the constituent quarks consists of various terms, which model the main symmetries and the dynamical content of QCD in the low-energy region. The spontaneous breakdown of chiral symmetry leads to the appearance of the pion as Goldstone boson and its chiral partner, the sigma meson. The coupling of these mesons to the constituent quarks is described in lowest order by the one-pion- (V^{OPEP}) and the one-sigma meson (V^{OSEP}) exchange potentials. The short-range part of the quark-quark interaction is mainly described by a one-gluon exchange potential (V^{OGEP}) . Finally, we model the quark confinement by a phenomenological two-body harmonic oscillator potential (V^{conf}) . Explicit expressions for the interaction terms may be found for example in Ref.[13].

For the orbital part of the wavefunctions we use unmixed harmonic oscillator eigenfunctions. Explicit expressions for the orbital wavefunctions are given in Ref.[16].

In the χ QPM we have six independent parameters. These are the constituent quark mass m_q , the quark-gluon coupling constant α_s , the oscillator parameter b and the confinement strength a_c . In addition, one should think of constituent quarks as extended particles with finite hadronic and electromagnetic size. Therefore, we introduce a cut-off parameter Λ in the one-pion and one-sigma meson exchange potentials. This cut-off results in extended quark-pion and quark-sigma meson vertices and can be interpreted in terms of a finite hadronic size of the quarks. The finite e.m. size of the constituents $r_{\gamma q}$ is parametrized by a monopole form factor which is multiplied with the one- and two-body current densities as described in Refs.[12] and [13]. We assume that the pion-photon and quark-photon vertices are parametrized by one and the same monopole form factor as discussed in Ref.[14]. In this way, the continuity equation for the e.m. current is still fulfilled.

The set of parameters used here is listed in Table 1. We chose a value of $r_{\gamma q}$ =0.6 fm which is compatible with a prediction of the simplest vector meson dominance model [17]. The way how the other parameters are determined is explained in Ref.[12].

Table 1

The coupling of the pion and the sigma meson to the quarks and the sigma meson mass are fixed according to the chiral symmetry arguments of Refs.[18] and [19]:

$$\frac{g_{\sigma q}^2}{4\pi} = \frac{g_{\pi q}^2}{4\pi} = \left(\frac{3}{5}\frac{m_q}{m_N}\right)^2 \frac{g_{\pi N}^2}{4\pi}, \qquad m_\sigma^2 = 4m_q^2 + \mu^2 \ . \tag{2}$$

Here $m_N = 939$ MeV is the nucleon mass and $\mu = 138$ MeV the pion mass. Furthermore, we chose $g_{\pi N}^2/4\pi = 13.845$.

In order to calculate electromagnetic properties of baryons, we have to know the four-vector current density $j_{\mu} = (\rho(x), -\mathbf{j}(x))$ of the interacting quarks in the baryon system. In the past, most calculations were done in the so-called impulse approximation, where a pure one-body current was used and two-body currents were neglected. However, a baryon is a strongly correlated system with strong interactions between the three constituents. Thus, it is intuitively clear that this simple description of the photon absorption process is incomplete. In fact, it has been shown that two-body currents are necessary to guarantee electromagnetic current conservation [12]. The complete current density (\mathbf{j}_{tot}) is therefore given by a sum of one-and two-body operators:

$$\mathbf{j}_{tot}(\mathbf{q}) = \sum_{i=1}^{3} \mathbf{j}_{imp}(\mathbf{r}_i) + \sum_{i < j=1}^{3} (\mathbf{j}_{g\overline{q}q}(\mathbf{r}_i, \mathbf{r}_j) + \mathbf{j}_{\pi\overline{q}q}(\mathbf{r}_i, \mathbf{r}_j) + \mathbf{j}_{\gamma\pi\pi}(\mathbf{r}_i, \mathbf{r}_j) + \mathbf{j}_{conf}(\mathbf{r}_i, \mathbf{r}_j) + \mathbf{j}_{\sigma\overline{q}q}(\mathbf{r}_i, \mathbf{r}_j)) ,$$
(3)

where $\mathbf{j}_{imp}(\mathbf{r}_i)$ is the one-body current density operator and $\mathbf{j}_{q\bar{q}q}$ ($\mathbf{j}_{\pi\bar{q}q}$) corresponds to the current density due to one-gluon-(one-pion) exchange. In addition, we obtain currents from the scalar part of the interaction, namely from the confinement potential (\mathbf{j}_{conf}) and the one-sigma meson exchange ($\mathbf{j}_{\sigma\bar{q}q}$). For the pion we get an additional part ($\mathbf{j}_{\gamma\pi\pi}$) from the pion-in flight diagram (Fig.1(c)) describing the photon coupling to the exchanged pion. The one-and two-body current densities may be obtained by a nonrelativistic expansion of the Feynman amplitudes of the diagrams displayed in Fig.1. Alternatively, the various contributions may be calculated by minimal substitution in the corresponding interaction terms of the χ QPM Hamiltonian. Explicit expressions for the one- and two-body operators may be found in Ref.[12]. Note, that the parameters for the present calculation of electromagnetic excitation

amplitudes are the same as the ones used for the calculations of the e.m. properties of the nucleon and $\Delta(1232)$ [13-15] and that we have not introduced any further parameters.

Figure 1

The electromagnetic excitation of the nucleon is determined by the photon-baryon interaction Hamiltonian

$$H_{em} = \int d^4x J_{\mu}(x) A^{\mu}(x) . {4}$$

The quantities which are usually extracted from photo pionproduction experiments are the so-called helicity amplitudes. For the excitation with real photons we only need the transverse helicity amplitudes defined by [3]

$$A_{\lambda}^{N} = -e\sqrt{\frac{2\pi}{\omega}}\langle B^{*}, \lambda \mid \boldsymbol{\epsilon} \cdot \mathbf{j}(\mathbf{q}) \mid N, \lambda - 1 \rangle .$$
 (5)

They describe the transition of the nucleon with total angular momentum projection $J_z = \lambda - 1$ to a resonance with total angular momentum projection $J_z = \lambda$ through the absorption of a photon with positive helicity. Here, ω is the energy transfer of the photon in the center of mass frame and ϵ is the photon polarization.

The transverse helicity amplitudes may be expressed in terms of electromagnetic multipole transition amplitudes. For this one decomposes the three-vector current density into electric and magnetic multipole operators [20],

$$j_m(\mathbf{q}) = -\sqrt{2\pi} \sum_{J=1}^{\infty} i^J \sqrt{2J+1} \left[m T_m^{[M]J}(q) + T_m^{[E]J}(q) \right]$$
 (6)

with $m=0,\pm 1$ being the three-vector current density components in the spherical basis. Because of the selection rules due to parity and angular momentum conservation, only a few multipole operators contribute. The $J=\frac{3}{2}$ resonances with positive parity, namely the $P_{33}(1232)$ and $P_{33}(1600)$, are excited by M1 and E2 multipoles while the $P_{11}(1400)$ is excited by M1 radiation only. Similarly, for the negative parity excitations the $S_{11}(1535)$ is excited by E1 radiation while the $D_{13}(1520)$ resonance can be reached by E1 and M2 transitions.

In Table 2, we give the results for the photocouplings of the positive parity resonances of the nucleon. For the helicity amplitudes, we use the same phase convention as Koniuk and Isgur [5]. The $P_{33}(1232)$ and the $P_{11}(1440)$ excitations have already been discussed in previous works [14,15], but now the helicity amplitudes are calculated for finite $|\mathbf{q}| = \omega$. Therefore, the e.m. size of the constituent quarks contributes. The finite e.m. size of the constituent quarks has already been shown to be important for the proton charge radius [12] and for the magnetic radii of the baryon octet [12,13]. Furthermore, we show in Table 2 our results for the $P_{33}(1600)$ resonance. For the Δ -isobar and its orbital excitation $P_{33}(1600)$, the results for the proton and neutron helicity amplitudes are identically the same. We see that for all resonances the contributions from the two-body currents are important. This especially holds for the confinement current which in some cases gives a 60%-contribution relative to the one-body current. In comparison with our results in Ref. [14] and [15], we obtain smaller excitation amplitudes due to the finite e.m. size of the constituents. Thus, for the Δ -isobar we are not able to improve our previous results [14,15] which deviate by 30-40% from experimental values. This difference is even slightly enlarged by the twobody currents and the finite e.m. size of the quarks. Another difference compared with our previous calculations in Refs.[14] and [15] arises from the different treatment of the E2 transition amplitude. In Refs.[14] and [15] we calculated the E2 amplitude with the charge density in the long-wavelength limit [10] which leads to a relation between transverse electric

and Coulomb transition amplitudes. Here, however, the E2 amplitude is calculated using the current density, which yields a vanishing E2 amplitude with unmixed harmonic oscillator wavefunctions.

In contrast to the $\Delta(1232)$, for the Roper resonance, as already discussed in [15], the two-body contribution tends in the right direction. However, in our previous calculations [15] the total amplitude came out too large. This is now improved by taking into account the finite e.m. size of the constituent quarks. For the Roper resonance, by virtue of the two-body contributions and the finite e.m. size, our new results are in better agreement with the experimental values than the results of the pure impulse approximation are.

As in the case of the Roper resonance, the exchange current contributions to the $P_{33}(1600)$ resonance reinforce each other. The $P_{33}(1600)$ excitation is only a $(\star \star \star)$ -resonance and the experimental data are less reliable. We obtain a good description of the $A_{1/2}$ amplitudes, but for the $A_{3/2}$ amplitudes a major difference between the calculated and experimental values, which is even enlarged by the two-body contributions.

Table 2

Looking at the negative parity resonances (Table 3), we again find that the two-body currents and especially the confinement current give important contributions to the helicity amplitudes. For the $S_{11}(1535)$ we obtain that the individual two-body contributions add constructively. For the neutron excitation, we get after including the two-body currents a similar good agreement with the experimental value as in impulse approximation. For the proton target, we obtain the interesting result that the helicity amplitude of the proton excitation to the $S_{11}(1535)$ resonance is strongly damped by the two-body amplitudes. Thus, after adding two-body operators to the current density the long-standing problem that non-relativistic quark model calculations considerably overestimate the proton excitation to the $S_{11}(1535)$ resonance [5], disappears. Our result is now in good agreement with experimental values from Ref.[21].

For the $D_{13}(1520)$ excitation amplitudes, we observe, in contrast to the $S_{11}(1535)$, at least for the $A_{3/2}$ amplitude cancellations of the individual two-body amplitudes. For the $A_{1/2}$ amplitude of the proton, the agreement with experiment is improved whereas the difference between the calculated $A_{3/2}$ amplitudes and the experimental values cannot be reduced.

We have listed in Tables 2 and 3 the contributions from the different multipole operators separately. For the Δ -isobar and the $P_{33}(1600)$, the E2 amplitude is zero (Table 2). For the D_{13} -excitation (Table 3), neither the E1 nor the M2 amplitude dominates the photoexcitation amplitudes. In order to further investigate the remaining differences between experimental extractions and our calculations of the $A_{3/2}$ amplitudes for the D_{13} excitation and of corresponding amplitudes for the Δ -isobar, a detailed study of the χ QPM Hamiltonian with perturbed harmonic oscillator wavefunctions should be made.

Table 3

Finally, we would like to concentrate on the pion-in-flight contribution (Fig.1(c)) whose importance has been discussed by several groups, recently. First, Robson [9] considered the effect of pion exchange currents in the photoproduction of several resonances. For the pion pair contribution, we agree with his calculations for the positive parity resonances if we consider a zero e.m. size of the constituents and a pointlike quark-pion vertex. However, Robson claimed that the pion-in-flight contributions are not significant for all excitations he studied and neglected them. This opinion is later joined by Perazzi et.al. in a new calculation [22]. In contrast, we get for the positive parity resonances important contributions from the pion-in-flight term. For the positive parity excitations, the pion-in-flight amplitude is even larger than the one from the pion-pair current. However, the two contributions from the pion are of different sign and therefore the total effect of the pion as the sum of both is

comparatively small, as has already been pointed out in Ref.[14] for the case of the Δ . Therefore, previous calculations [9,22] that neglected the pion-in-flight term for positive parity excitations considerably overestimated the pion exchange current contributions. For the negative parity resonances, the amplitude from the pion-in-flight current is not as large as the one from the pion pair current, but again it gives, at least with our usual set of parameters of Table 1, non-negligible contributions. Looking at the contributions of different multipole operators to the total pion-in-flight amplitude, we realize that for the $P_{33}(1232)$ and the $P_{33}(1600)$ the total amplitude is given by the M1 multipole operator whereas for the $D_{13}(1520)$ only the E1 operator contributes. The E2 and M2 amplitudes vanish due to the spin-isospin structure of the wavefunctions. Therefore, one has to properly take into account the pion-in-flight contributions.

Summarizing, we calculated the photoexcitation amplitudes of all nucleon resonances up to $\sqrt{s} = 1.6$ GeV. We observed that exchange current contributions, and especially the confinement current, give significant contributions for the helicity amplitudes of all nucleon resonances. For the $P_{11}(1440)$ and the $S_{11}(1535)$, we get an improvement with respect to the impulse approximation. This, however, does not hold as a general tendency. For example, for the $P_{33}(1232)$ or the $D_{13}(1520)$, we are not able to get a better agreement with the data.

In a future work, the baryon orbital wavefunctions should be expanded in a larger Hilbert space. In addition, due to its importance for the e.m. production of nucleon resonances, the phenomenological confinement potential should be examined in more detail. In particular, different radial forms (linear, color-screened, ...) should be studied concerning their effect both on the baryon spectrum and e.m. transition amplitudes.

Acknowledgment: We would like to thank B. Krusche and W. Pfeil for fruitful discussions.

References

- [1] Volker D. Burkert, Czech. J. Phys. 46 (1996) 627
- [2] C.M. Becchi and G. Morpurgo, Phys. Lett. 17 (1965) 352
- [3] L.A. Copley, G. Karl and E. Obryk, Nucl. Phys. **B13** (1969) 303
- [4] T. Kubota and K. Ohta, Phys. Lett. 65B (1976) 374
- [5] Roman Koniuk and Nathan Isgur, Phys. Rev. **D21** (1980) 1868
- [6] Frank E. Close, Zhenping Li, Phys. Rev. **D42** (1990) 2194
- [7] W. Warns, H. Schröder, W. Pfeil, H. Rollnik, Z. Phys. C45 (1990) 627
- [8] Simon Capstick, Phys. Rev. **D46** (1992) 2864
- [9] D. Robson, Nucl. Phys. **A560** (1993) 389
- [10] A.J.F. Siegert, Phys. Rev. **52** (1937)
- [11] A.J. Buchmann, E. Hernández and K. Yazaki, Phys. Lett. **B269** (1991) 35
- [12] A.J. Buchmann, E. Hernández, K. Yazaki, Nucl. Phys. **A569** (1994) 661
- [13] Georg Wagner, A.J. Buchmann and Amand Faessler, Phys. Lett. **B359** (1995) 288
- [14] A.J. Buchmann, E. Hernández and Amand Faessler, Phys. Rev. C55 (1997) 448
- [15] A.J. Buchmann, U. Meyer, E. Hernández, and Amand Faessler, Acta Phys. Pol. B27 (1996) 3161
- [16] M.M. Giannini, Rep. Prog. Phys. **54** (1990) 453
- [17] U. Vogl, M. Lutz, S. Klimt and W. Weise, Nucl. Phys. **A516** (1990) 469
- [18] I.T. Obukhovsky and A.M. Kusainov, Phys. Lett. **B228** (1990) 142
- [19] F. Fernández, A. Valcarce, U. Straub, and Amand Faessler, J. Phys. G19 (1993) 2013
- [20] T. DeForest, Jr. and J.D. Walecka, Advances in Physics 15 (1966) 1
- [21] Particle Data Group, Phys. Rev. **D54** (1996) 569
- [22] E. Perazzi, M. Radici and S. Boffi, Nucl. Phys. A614 (1997) 346

$m_q [{ m MeV}]$	b [fm]	α_s	$a_c [\mathrm{MeV \cdot fm^{-2}}]$	$\Lambda \; [\mathrm{fm}^{-1}]$	$r_{\gamma q}$ [fm]
313	0.613	1.093	20.92	4.2	0.6

Table 1: Quark model parameters

		A_i	A_g	$A_{\pi q \bar{q}}$	$A_{\gamma\pi\pi}$	A_c	A_{σ}	A_{tot}	exp. [21]
$P_{33}(1232)$	$A_{1/2}(M1)$	-94	-10	+15	-18	+36	-11	-82	
	$A_{1/2}(E2)$	0	0	0	0	0	0	0	
	$A_{1/2}(tot)$	-94	-10	+15	-18	+36	-11	-82	-140 ± 5
	$A_{3/2}(M1)$	-163	-17	+26	-31	+62	-19	-142	
	$A_{3/2}(E2)$	0	0	0	0	0	0	0	
	$A_{3/2}(\text{tot})$	-163	-17	+26	-31	+62	-19	-142	-258 ± 6
$P_{11}(1440)$	$A_{1/2}^{p}(M1)$	-30	-16	+5	-13	-21	-15	-90	-65 ± 4
	$A_{1/2}^{n'}({ m M1})$	+20	+5	-8	+13	+14	+10	+54	$+40\pm10$
$P_{33}(1600)$	$A_{1/2}(M1)$	-19	-4	+5	-8	-4	-7	-37	
	$A_{1/2}(E2)$	0	0	0	0	0	0	0	
	$A_{1/2}(tot)$	-19	-4	+5	-8	-4	-7	-37	-23 ± 20
	$A_{3/2}(M1)$	-33	-7	+8	-14	-6	-12	-64	
	$A_{3/2}(E2)$	0	0	0	0	0	0	0	
	$A_{3/2}(tot)$	-33	-7	+8	-14	-6	-12	-64	-9 ± 21

Table 2: Helicity amplitudes for the $\gamma N \to P_{33}(1232), P_{11}(1440), P_{33}(1600)$ transitions in units of GeV^{-1/2} × 10⁻³ with the parameters of Table 1 evaluated at $|\mathbf{q}_{c.m.}| = \omega_{c.m.}$. $A_i = \text{impulse}, A_g = \text{gluon}, A_{\pi q \bar{q}} = \text{pion pair}, A_{\gamma \pi \pi} = \text{pion-in-flight}, A_c = \text{confinement},$ and $A_{\sigma} = \text{sigma}$ meson contributions. A_{tot} is the sum of all contributions. The proton and neutron transition amplitudes to the $P_{33}(1232)$ and $P_{33}(1600)$ resonances are the same. The M1 and E2 contributions are given separately.

		A_i	A_g	$A_{\pi q \bar{q}}$	$A_{\gamma\pi\pi}$	A_c	A_{σ}	A_{tot}	exp. [21]
$D_{13}(1520)$	$A_{1/2}^{p}(E1)$	+19	+6	-9	-1	+11	-2	+24	
	$A_{1/2}^{p'}(M2)$	-63	-11	0	0	+34	-4	-44	
	$A_{1/2}^{\not p}(\mathrm{tot})$	-44	-5	-9	-1	+45	-6	-20	-24 ± 9
	$A_{1/2}^{n}(E1)$	-33	-8	+9	+1	-4	+1	-34	
	$A_{1/2}^{n'}(M2)$	+21	+5	0	0	-11	+1	+16	
	$A_{1/2}^{n}(\text{tot})$	-12	-3	+9	+1	-15	+2	-18	-59 ± 9
	$A_{3/2}^p(E1)$	+32	+10	-16	-2	+19	-2	+41	
	$A_{3/2}^{p'}(M2)$	+37	+6	0	0	-19	+2	+26	
	$A_{3/2}^{p'}(\text{tot})$	+69	+16	-16	-2	0	0	+67	$+166 \pm 5$
	$A_{3/2}^n(E1)$	-57	-13	+16	+2	-6	+1	-57	
	$A_{3/2}^n(M2)$	-12	-3	0	0	+6	-1	-10	
	$A_{3/2}^{n}(\text{tot})$	-69	-16	+16	+2	0	0	-67	-139 ± 11
$S_{11}(1535)$	$A_{1/2}^{p}(E1)$	+114	-16	-13	-2	-31	+4	+56	$+70\pm12$
	$A_{1/2}^{n'}(E1)$	-74	+20	+13	+2	+10	-1	-30	-46 ± 27

Table 3: Helicity amplitudes for the $\gamma N \to D_{13}(1520)$ and $S_{11}(1535)$ transitions in units of $\text{GeV}^{-1/2} \times 10^{-3}$ with the parameters of Table 1 evaluated at $|\mathbf{q}_{c.m.}| = \omega_{c.m.}$. $A_i = \text{impulse}$, $A_g = \text{gluon}$, $A_{\pi q\bar{q}} = \text{pion pair}$, $A_{\gamma\pi\pi} = \text{pion-in-flight}$, $A_c = \text{confinement}$, and $A_{\sigma} = \text{sigma meson contributions}$. A_{tot} is the sum of all contributions. The E1 and M2 contributions are given separately.

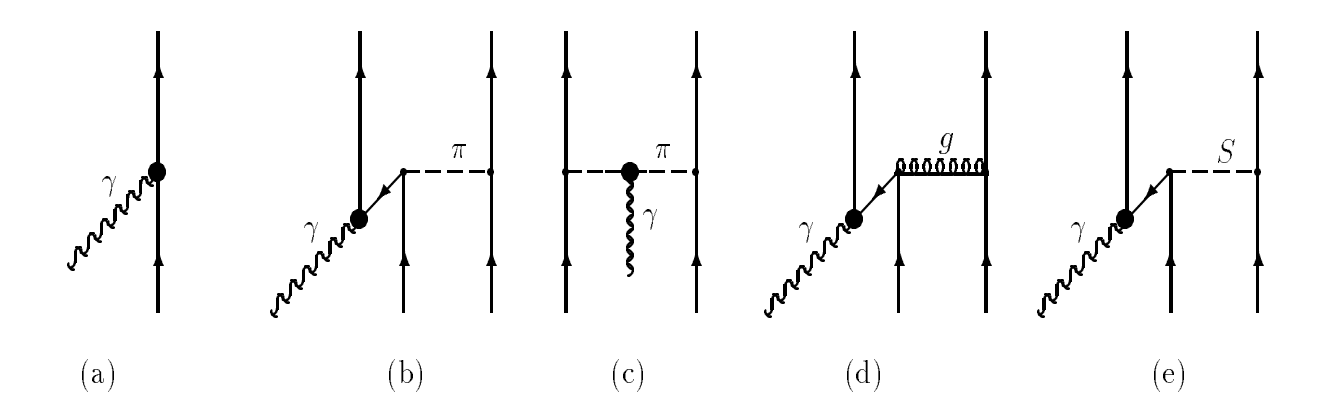


Figure 1: One-body and two-body exchange currents between quarks: (a) impulse, (b) pion pair, (c) pion-in-flight, (d) gluon pair, (e) scalar pair, i.e. σ meson or confinement pair.